Fall 2020

Analysis of Semi-Arid Riparian Environments using Satellite Imagery

Kira Overin

Kira Overin

Non-Thesis Project

Analysis of Semi-Arid Riparian Environments using Satellite Imagery

Fall 2020

ABSTRACT

Semi-arid riparian environments are at risk of being over-exploited or degraded due to increased water usage associated with growing housing demands. Trends surrounding these developments can be monitored using freely available Landsat satellite imagery in conjunction with seasonal stream discharge rates. This project focuses on a stream system located southwest of Ennis, Montana, where population is growing rapidly. It aims to characterize the connection between variable discharge rates in small-scale riparian environments and adjoining vegetation health, while considering possible implications of continued urbanization. Methods for preventing riparian ecosystem degradation and promoting resilience are also discussed.

TABLE OF CONTENTS

TABLE OF FIGURES

Introduction

Increased urbanization is a phenomenon affecting nearly all majorly populated areas of the Earth, with projections showing that growth of previously sparsely or unsettled areas are expected to increase in population and be made into new housing developments (Alig, Kline, & Lichtenstein, 2004). Recently, teleworking has become a viable option for more workers than ever before, offering the choice of living remotely from the workplace (Pérez-Pérez et al., 2004). People who once were required to live nearby their office may now have the opportunity to move away from densely populated cities into more rural settings while maintaining their current occupation by working remotely. With the prospect of cities becoming less centralized and populations more dispersed, an increase in new housing developments must be expected. In order to proactively anticipate increased urbanization in rural areas, several factors should be addressed including protecting the original landscape, hydrologic systems, wildlife, and other natural processes that rely on the continued balance between one another.

An example of rapidly increasing urbanization can be found in Ennis, Montana, which has seen a nearly 20% increase in population in the last ten years alone (United States Census Bureau, 2020). One particular new housing development currently being established consists of 135 individual lots for purchase, each with its own well and septic system. Tight groupings of individual pumping wells such as this can over-stress an aquifer, resulting in decreased groundwater availability, storage, and could eventually lead to ground subsidence (Odeh et al., 2019). The emergent housing developments are situated on the southwestern side of the Madison River on semi-arid grasslands receiving less mountain front due to the relatively diminutive size of the mountain above (Viviroli et al., 2007). Before a system becomes over-exploited, it's

essential to understand the intact system, including surface water seasonal fluctuations and trends, as well as local vegetation density and variance.

The goals of the project include the use of satellite imagery in the Eightmile Creek watershed near Ennis, MT to i) establish a baseline of how vegetation changes associated with variable stream discharge prior to urbanization, and ii) make predictions and recommendations to minimize negative impacts from subdividing in semi-arid regions. Images captured by the Landsat 7 and 8 satellites were processed and used to find NDVI values to reflect vegetation health changes associated with seasonal flows, along with considering possible impacts of continued urbanization.

Charles Shama previously completed a study in the area in 2018, which discussed parameters that may affect groundwater recharge and stream flows including local and regional geology, precipitation infiltration, and mountain front recharge (Shama, 2018). This study used isotopes, specific conductivity, and water temperature to identify gaining and losing reaches of two local streams, as well as relative contributions to these systems from snowmelt and groundwater. Using end member mixing models, specific conductivity, and local meteoric water lines, he was able to conclude that groundwater consistently contributes to local streams within the mountains but continually recharges shallow aquifers along the benches. The largest amount of recharge is during snowmelt. The mountain front/bench boundary changes from groundwater discharge to creeks during snowmelt, but groundwater recharge during the rest of the year. This study also highlights the importance of adequate snowmelt moving down through a system to recharge local aquifers.

Site Description

Climate

According to the Western Regional Climate Center, the climate in Ennis, Montana on average ranges from 23.0 and 64.4 degrees Fahrenheit found in December and July, respectively. The average precipitation is 12.49 inches per year, with 3.86 inches accumulating in spring, 4.79 inches falling in summer, and the remaining 3.84 inches falling in fall and winter (Western Regional Climate Center, n.d.). This particular area of Ennis is significant because while the current balance of the hydrological system affords residents consistent access to ground and surface water, it could become jeopardized by overextraction of ground water due to increased residential development.

Map of Study Area

The images shown in Figure 1 portrays a map of Montana with a red star situated where Ennis lies. The inset image shows an aerial image of Ennis along with a place marker where the study area lies, approximately four miles to the southwest. Below that is an aerial image of the study area displaying the eight sites relative to one another along the creek. The total distance from Site 1 to Site 8 is approximately 3.7 miles, following the stream. The channel flows from west to east, or left to right, as seen in the image below.

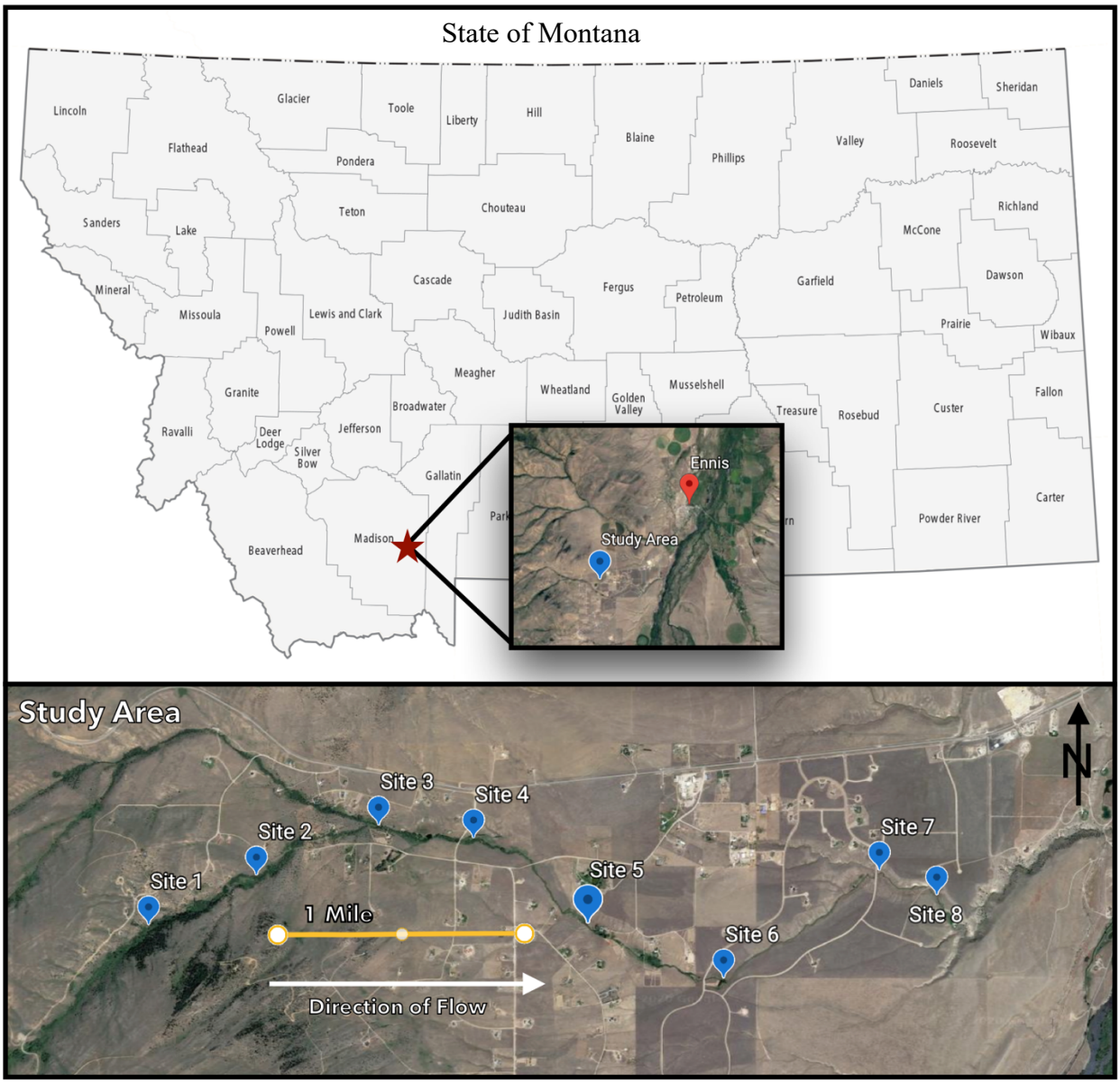

Figure 1. Map of Montana with county lines shown, followed by study area site map showing spacing and spatial relationship of eight sites on Eightmile Creek. (Google Earth, 2020).

Local Geology

Ennis lies within a structural basin created by surrounding fault zones, which result in an unevenly tilted bedrock underlayment of metamorphic Archean rocks dipping toward the east. The basin has since infilled with approximately 200 feet of unconsolidated sediments ranging

from silt to well-rounded boulder-sized clasts due to high energy river environments that have snaked through the basin over time, shown in Figure 2 (Kellog et al., 2007).

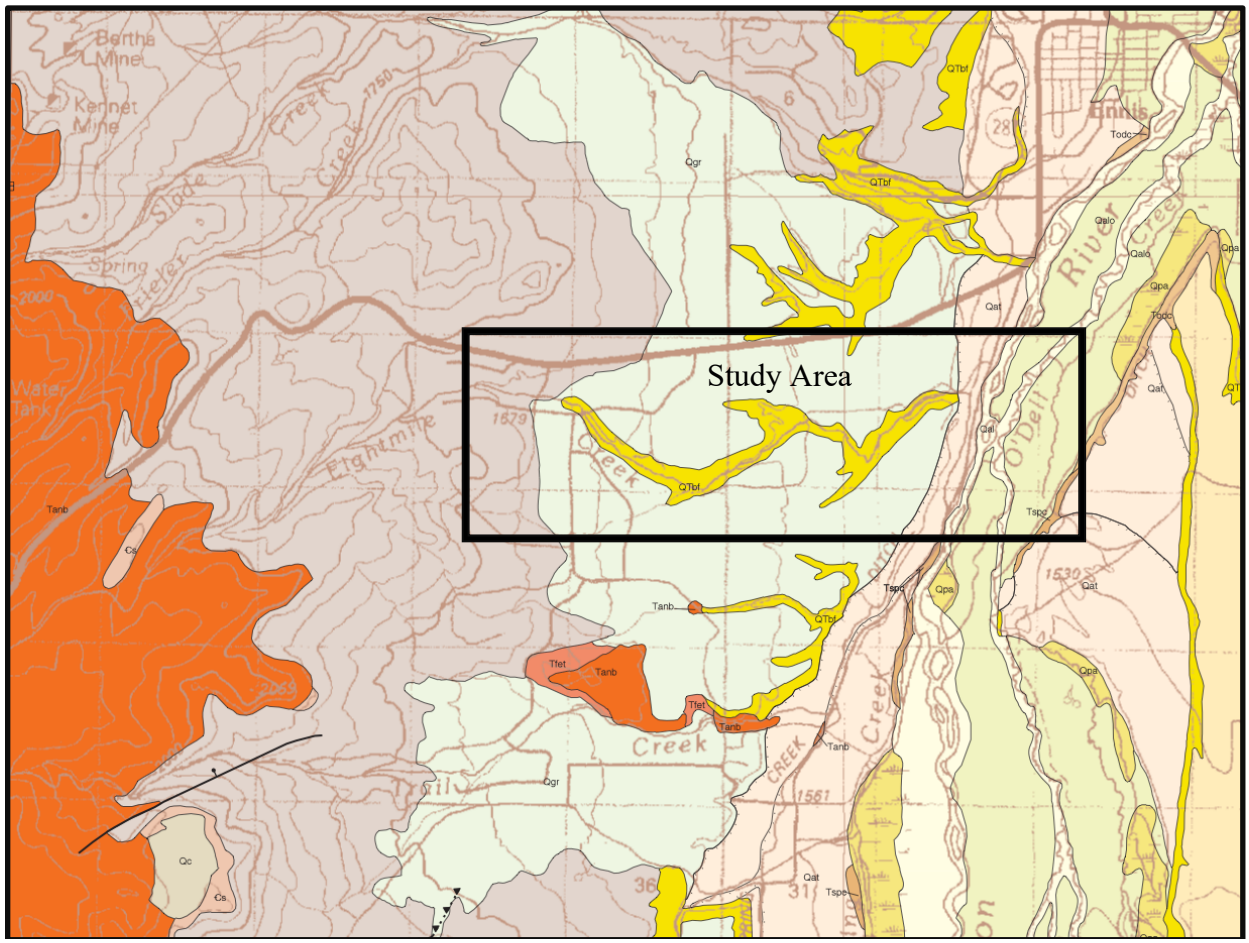

Figure 2. Regional geology map of southwest section of Ennis, Montana from the Montana Bureau of Mines and Geology. (Edited from Kellog et al., 2007).

Eightmile Creek has been moderately disturbed, with several houses build near its banks, and several ponds built on or near it as well. Each of the residences present in the area have a well for domestic use including household purposes and some minor outdoor irrigation. Based on well logs pulled from GWIC, the higher elevation sites, 15 to 80 feet of unconsolidated topsoil (depending on location and placement on slope) and decomposing granite overlays fractured granite followed by solid granite bedrock (Montana Bureau of Mines and Geology, 2020).

Vegetation present surrounding Eightmile Creek consists of shortgrass prairie varieties, most commonly dominated by bluebunch wheatgrass (*Pseudoroegneria spicata*), and Idaho fescue (*Festuca idahoensis*), big sagebrush (*Artemisia tridentata*), Rocky Mountain juniper (*Juniperus scopulorum*) with some additional agricultural grasses including smooth brome (*Bromus inermis*), Kentucky blue grass (*Poa pratensis*), orchard grass (*Dactylis glomerata*), and canary reed grass (*Phalaris arundinacea*) growing very near the banks and thinning where water is not immediately available (Mueggler & Stewart, 1980). Reaches of higher elevation which fosters additional vegetation growth compared to the lower elevation, unshaded counterparts, present increased density of conifer species including lodgepole pine (*Pinus contorta*), Douglass fir (*Pseudotsuga menziesii*), and other evergreen species. Closer to where Eightmile Creek meets the Madison River, there are very few trees present, with only a few cottonwoods and willows sparsely dotting the stream on or very near the channel.

Methods

Procedures and Site Descriptions

Data collection for the stream discharge used in this project began in July 2018 and continued through November 2019. Approximately 22 stream discharge measurements were taken at each of the sites over the course of 17 months, with some data points missing at sites due to weather, terrain, or issues with wildlife. No discharge measurements were taken during winter months because there is no flow at that time.

The eight sites can be categorized into three groups based on a combination of elevation and topographical characteristics, as summarized in Table 1. The first group (beginning from upstream and moving downstream), characterized by higher elevation, denser coniferous tree

cover and generally greener, fuller ground cover, is composed of Site 1, Site 2, Site 3, and Site 4. Site 1 is narrow with steep banks, and heavy vegetation interaction with plants growing directly in the water from the banks. Site 2 is approximately 180 feet lower in elevation than the Site 1 and is partially obscured by intermixed evergreen and deciduous trees and including various conifers, aspen, and juniper. Site 3 is an additional 195 feet lower in elevation and features an unlined pond downstream from the gauging station. The creek is located approximately ten feet down an embankment featuring a dense grove of aspen in the ditch, and mature sagebrush further from the banks. Site 4 is also in a grove of trees and is much smaller than other reaches of the creek, as it is measured after a flow diversion occurs. Flows on Site 4 were quite variable as the owners of the diversion would divert all or most of the water from one channel to the other based on the season. During the study period, water was diverted from the main channel to the secondary channel beginning around July and re-diverted back around September.

The mid-elevation sites include Site 5 and Site 6. Site 5 was partially spring fed, according to landowners. This site features a reduced tree density, with only limited cottonwoods nearby downstream, and no major vegetation present more than a few feet from the creek banks. Site 6 is similar to Site 5, except it is situated within a collection of mature cottonwood trees and has extensive vegetation growth surrounding the stream, possibly due shade provided by the trees and to the wider, more meandering nature of this sections of creek.

Finally, the lower elevation sites include the Site 7 and Site 8. Site 7 has no trees nearby, and only grows canary reed grass (*Phalaris arundinacea*) which promptly dies after the major rainy periods are over. Site 8 is similar, with no trees locally and only dense grass very near the creek. From Site 8, flows move into an unlined pond approximately 800 feet downstream where it is allowed to infiltrate. If flows are sufficient, the pond can fill and reach an outlet at the side of

the dam, where it flows into the next portion of Eightmile Creek and then into the Madison River, about a mile away.

Table 1 contains a summary of basic position information for each site, along with average channel width and common vegetation types found at each site.

	Elevation [ft]	*Latitude*	*Longitude*	*Avg. Channel Width [ft]*	*Predominant Vegetation*
Site 1	5959	45.3089	-111.8325	1.2	Deciduous, conifer, grass
Site 2	5773	45.3119	-111.8236	1.8	Deciduous, conifer, grass
Site 3	5578	45.314685	-111.81325	3.2	Mixed deciduous, grass
Site 4	5471	45.314013	-111.8058	1.4	Mixed deciduous, grass
Site 5	5358	45.308815	-111.79562	1.3	Cottonwood, grass
Site 6	5279	45.305605	-111.78415	3.6	Cottonwood, grass
Site 7	5183	45.312089	-111.77087	1.6	Grass only
Site 8	5151	45.309777	-111.76544	1.2	Grass only

Table 1. Eightmile Creek monitoring site characteristics

Field Methods

Stream Discharge

Stream velocity was measured using a Marsh-McBirney Flo-Mate electromagnetic flow meter mounted on a standard wading rod. The flow meter probe was submerged in the stream, parallel to flow, with the sensors facing upstream. The probe was kept submerged in place for approximately 20 seconds while the velocity was computed by the flowmeter. The velocity was then recorded by hand in a field notebook. This process was repeated in 0.2 to 0.4-foot increments until the entire width of the stream had been measured. Narrower sections of the stream necessitated more closely spaced measurement points, while wider areas allowed the points to be more spaced out. The goal for the spacing chosen was to have approximately 20 data points in each run so that there would not be more than 5 percent of the total discharge being measured between any two points. Due to the occasionally very narrow nature of Eightmile

Creek, several runs could not reach the full 20 points. Care was taken to avoid areas with especially turbulent flow, drastically narrowing or widening sections, and areas with large rocks or debris that could impede or significantly alter the velocity measurements. Data was then transferred into Microsoft Excel where it was manually entered into an Excel Macro containing the equations used to determine volumetric flow from velocity and stream dimensions. A sample of the equation can be found below.

Equation 1 $\textit{flow rate} = (t_c - t_p)/2*(d_c * v_c + d_p * v_p)$ *[cubic feet per second]*

where:

t_c = distance from bank at current station

t_p = distance from bank at previous station

d_c = depth of stream at current station

d_p = depth of stream at previous station

v = flow velocity

Percent of the total flow is also calculated at each station once the flow rate is calculated, using the following equation:

Equation 2 *(flow in section/total flow*100)* *[percent of total]*

This is used to help verify the validity of the measurement taken, as its recommended that no more than five percent of the total flow should be measured in any single station.

Analytical Methods

Normalized Difference Vegetation Index Description

Equation 3, shown below, reflects the bands and equation needed to find the Normalized Difference Vegetation Index, or NDVI, values in an image. This equation applies to Landsat 8

only, as each of the band labeling numbers have been shifted down one from those of Landsat 7 due to the addition of a new band in the Landsat 8 system.

Equation 3 $$NDVI = \frac{(Band\ 5 - Band\ 4)}{(Band\ 5 + Band\ 4)}$$

While the majority of the images in this study originated from the Landsat 8 satellite, several additional images were used that were captured by the Landsat 7 satellite due to availability of images without significant cloud cover. The equation for processing these images is the same however band designations are shifted by one. This means bands 4 and 3 are used in place of bands 5 and 4; no other changes are necessary.

NDVI provides a value indicating the greenness of vegetation using the ratio between red and near infrared light that is reflected and sensed by the instruments mounted on a satellite. This is a simple and useful indicator for general changes and trends in vegetation health, but it has some draw backs. NDVI values can be impacted by common atmospheric effects like presence of aerosols and clouds (U.S. Geological Survey, n.d.). Dense cloud cover makes an image visibly unworkable because it can completely obscure the land below, however images with heavy or unacceptable cloud cover can be filtered out of the results using the 'cloud cover' filtering feature within Earth Explorer.

The filtering criteria used for selecting all images was 15 to 20 percent or less cloud cover due to more consistent availability of these images. It's always preferable to use images with the smallest possible amount of cloud cover present, however it is not practical to exclude all images containing clouds, as there would likely be no remaining images to choose from. Therefore, when entering image search criteria, 15 percent cloud cover was chosen, and resulting images were selected. Cloud cover tolerance was then increased to 20 percent in an attempt to

find images taken during periods that previously did not produce an image under 15 percent coverage constraints. In the event that images for a time period were still not available, the next available image was then selected in its place, usually a few weeks before or after the desired time frame. An additional constraint regarding image availability are that there is not any overlap in images available for this particular study area. This means Ennis, Montana appears in images taken of one specific Path and Row (path 008, row 004) of the satellite imaging swath. All data for the satellite image processing portion of this project were collected from Earth Explorer, a data portal of the United States Geological Survey.

In order to produce NDVI value images, one must first retrieve images that have been processed from the original DN values recorded by the satellite's sensors into surface reflectance values, which can be obtained from Earth Explorer. Once surface reflectance images have been acquired, bands 4 and 5 (or 3 and 4 if using Landsat 7 images) must be isolated for NDVI calculations. Next, drag the raster layers into the Table of Contents window so that they can be used in the Raster Calculator function. Open the ArcToolbox and choose Spatial Analyst Tools > Map Algebra > Raster Calculator. Within the Raster Calculator dialogue, enter the equations discussed above to yield NDVI values using the relevant bands.

The primary analysis of NDVI images is very straightforward: areas that are brighter represent a greater ratio of red and near infrared light being reflected and received by the sensor, indicating the vegetation in the area is denser or healthier. These two bands are used to measure vegetation health because blue and red wavelengths are absorbed and used to produce energy during photosynthesis, while infrared and near infrared wavelengths are reflected by the leaves (Sabins, 2007). Healthier leaves reflect more near infrared light, while both healthy and

unhealthy reflect the same amount of red light. Therefore, measuring the relative differences in the ratios of these types of light produces a value indicating the health of the vegetation.

Results

Auxiliary Precipitation Data

In instances where additional data related to humidity, precipitation, snow fall, temperature, and other parameters are needed for an area, but are not covered by specific data collection methods used for the project, other sources of data must then be considered. For this project, five years of cumulative precipitation data were needed in order to establish variations in overall water availability for that year, and to be able to make comparisons year to year. Snow telemetry or SNOTEL sites are excellent sources for this type of information. The network is run by the National Water and Climate Center and consists of over 800 remote, high-elevation sites scattered throughout the western U.S. (National Water and Climate Center, n.d.).

Figure 3, shown below, contains five years of precipitation accumulation data for the Lower Twin SNOTEL site, located approximately 15 miles northwest of Ennis and the project area, at an elevation of 7900 ft. According to these data sets, the 2017 water year had the most precipitation, with a total of 46.2 inches accumulating. The year with the least total precipitation was the 2015 water year, with only 37.6 inches total. On average, the last five water years resulted in 40.7 inches of precipitation.

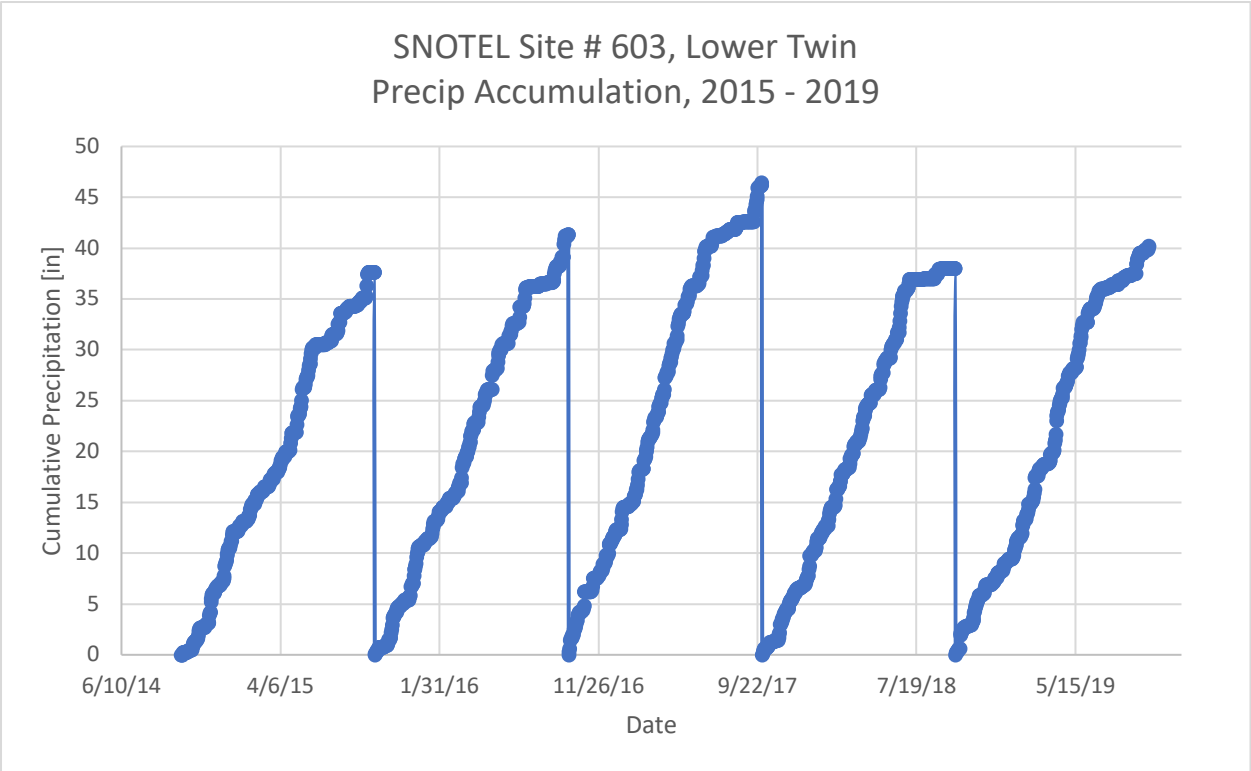

Figure 3. SNOTEL Site #603, Lower Twin

NDVI By Site Comparison Data

The following graph, Figure 4 , displays NDVI values of all sites for all five study years. The color scheme chosen reflects placement on stream, and therefore elevation. The darkest green lines represent Site 1, and the following lines represent each site as they are situated on the steam, each site represented in lighter green based on their position downstream, until finally reaching Site 8, shown in very pale green. This graphic helps to convey the trend of photosynthetic rates decreasing as one moves downstream. These are discrete values, with data only at the points shown, however lines connecting one point to the next were added for ease of viewing. These are not meant to represent NDVI values in between data points, especially during winter months.

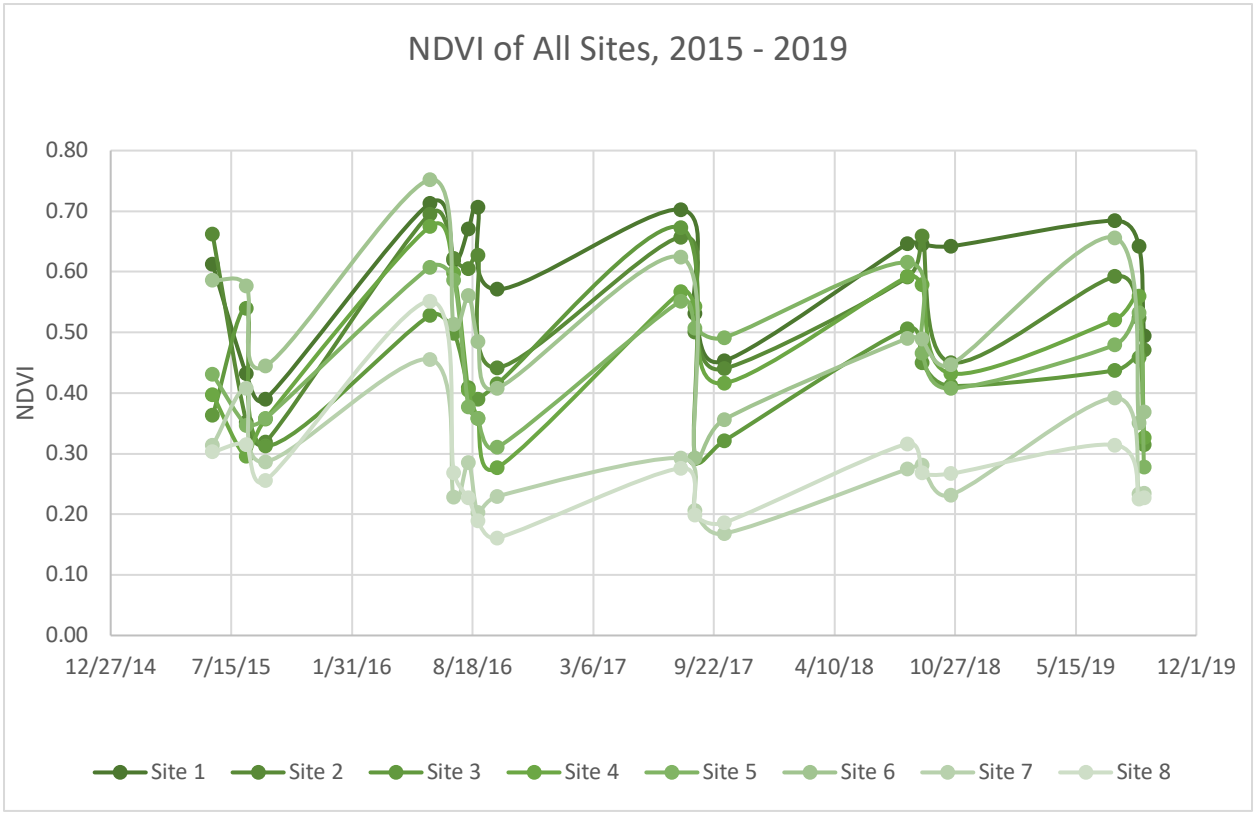

Figure 4. NDVI data for all sites displaying intensity of NDVI values of sites based on location on stream.

Stream Discharge Data

As described previously, stream flow velocity was monitored using a Marsh-McBirney Flo-Mate electromagnetic flow meter, coupled with stream profile dimensions, resulting in a volumetric flow rate calculated for each site every two weeks, excluding winter. Since 15 to 20 minutes are required per site, flow rates reflect average flows during that 15-to-20-minute window. Staff gauge measurements were taken before and after each transect to ensure no major changes occurred while readings were taken.

Table 2 contains all stream discharge measurements taken at eight sites along Eightmile Creek between the dates of July 31, 2018 through November 5, 2018, and April 18, 2019 through November 7, 2019.

Table 2. Stream discharge data for 2018 and 2019 of Eightmile Creek in Ennis, Montana.

	Site 1	**Site 2**	**Site 3**	**Site 4**	**Site 5**	**Site 6**	**Site 7**	**Site 8**	***Units***
11/7/19	0.13	0.17	0.54	0.43	0.43	0.9	0.6	0.74	CFS
10/31/19	0.12	0.18	0.48	0.39	0.16	0.46	0.54	0.49	CFS
10/8/19	0.11	0.29	0.55	0.1	0.16	0.41	0.49	0.46	CFS
9/17/19	0.09	0.16	0.56	0.04	0.16	0.5	0.31	0.35	CFS
8/26/19	0.09	0.2	n/a	0.06	0.16	0.3	0.33	0.38	CFS
8/13/19	0.18	0.23	n/a	0.12	0.38	0.83	0.74	0.76	CFS
7/29/19	0.11	0.23	0.51	0.1	0.25	0.51	0.49	0.43	CFS
7/16/19	0.17	0.32	0.65	0.25	0.36	0.46	0.55	0.5	CFS
6/30/19	0.16	0.25	0.53	0.19	0.52	0.64	0.48	0.43	CFS
6/19/19	0.22	0.29	0.7	0.22	0.43	0.52	0.48	0.5	CFS
5/29/19	0.19	0.29	0.74	0.44	0.61	0.56	0.49	0.56	CFS
5/15/19	0.34	0.35	0.85	0.52	0.67	0.69	0.59	0.58	CFS
5/4/19	0.4	0.31	0.64	0.52	0.46	0.74	0.52	0.46	CFS
4/18/19	0.23	0.3	0.77	0.28	0.3	0.62	0.39	0.24	CFS
11/5/18	0.13	0.16	0.29	0.29	0.16	0.19	0.29	0.18	CFS
10/22/18	0.1	0.15	0.3	0.3	0.2	0.17	0.17	0.16	CFS
10/7/18	0.1	0.13	0.3	0.28	0.1	0.15	0.11	0.13	CFS
9/24/18	0.08	0.1	0.32	0	0.11	0.13	0.08	0.08	CFS
9/10/18	0.07	0.1	0.23	0.011	0.13	0.17	0.09	0.07	CFS
8/27/18	0.17	0.17	0.37	0.005	0.1	0.11	0.12	0.12	CFS
8/13/18	0.08	0.14	0.21	0	0.08	0.07	0.17	0.12	CFS
7/31/18	0.1	0.2	0.34	0.012	0.2	0.38	0.16	0.13	CFS
7/17/18	0.09	0.26	0.5	0.052	0.25	0.4	0.29	0.23	CFS

Table 3 contains all of the NDVI values obtained from a total of 17 satellite images, from which 136 NDVI datapoints were acquired. The values are arranged by site and date that the image was captured. Because NDVI values are normalized and a ratio, they are unitless.

NDVI Data

Table 3. NDVI values retrieved from Landsat 7 and 8 images after processing.

	Site 1	**Site 2**	**Site 3**	**Site 4**	**Site 5**	**Site 6**	**Site 7**	**Site 8**	***Satellite***
6/14/15	0.61	0.66	0.36	0.40	0.43	0.59	0.31	0.30	Landsat 7
8/9/15	0.43	0.35	0.54	0.30	0.35	0.58	0.41	0.31	Landsat 8
9/10/15	0.39	0.32	0.31	0.36	0.36	0.44	0.29	0.26	Landsat 8
6/8/16	0.71	0.70	0.53	0.67	0.61	0.75	0.46	0.55	Landsat 8
7/18/16	0.62	0.62	0.50	0.60	0.59	0.51	0.23	0.27	Landsat 7
8/11/16	0.67	0.60	0.41	0.40	0.38	0.56	0.29	0.23	Landsat 8
8/27/16	0.71	0.63	0.39	0.36	0.36	0.48	0.20	0.19	Landsat 8
9/28/16	0.57	0.44	0.41	0.28	0.31	0.41	0.23	0.16	Landsat 8
7/29/17	0.70	0.66	0.67	0.57	0.55	0.62	0.29	0.28	Landsat 8
8/22/17	0.53	0.50	0.29	0.54	0.51	0.29	0.21	0.20	Landsat 7
10/9/17	0.45	0.44	0.32	0.42	0.49	0.36	0.17	0.19	Landsat 7
8/9/18	0.65	0.59	0.51	0.59	0.62	0.49	0.27	0.32	Landsat 7
9/2/18	0.64	0.66	0.45	0.58	0.47	0.49	0.28	0.27	Landsat 8
10/20/18	0.64	0.45	0.41	0.43	0.41	0.45	0.23	0.27	Landsat 8
7/19/19	0.68	0.59	0.44	0.52	0.48	0.66	0.39	0.31	Landsat 7
8/28/19	0.64	0.52	0.46	0.56	0.53	0.35	0.23	0.22	Landsat 8
9/5/19	0.49	0.47	0.32	0.33	0.28	0.37	0.23	0.23	Landsat 8

Discharge and NDVI Values by Site and Year

The following graphs compare yearly stream discharge rates and NDVI values calculated at each site. The descriptions begin with Site 1, at the upper-most location on Eightmile Creek, and concludes on Site 8, which is the furthest downstream. NDVI values (second y-axis axes) are all set to range from 0 to 1. Discharge value (y-axis) are scaled to best fit 2018 and 2019 data for each site, meaning graphs for both years at each site are identical to allow visual comparison of slope and data trends.

Site 1

Figure 5 shows a generally stable flow rate throughout the study period (July through October) at Site 1, ranging from 0.09 CFS to 0.18 CFS. The NDVI values followed suit, with values holding steady at 0.64 to 0.65. Figure 66 shows a maximum discharge in May in 2019, followed by a continuous decrease, finding the lowest flows in mid-September. NDVI values follow this downward slope, displaying a decrease in surrounding vegetation greenness as flows decrease. This follows the narrative that Site 1 tends to maintain a steady environment throughout the summer, with a gentle decline as the summer months close.

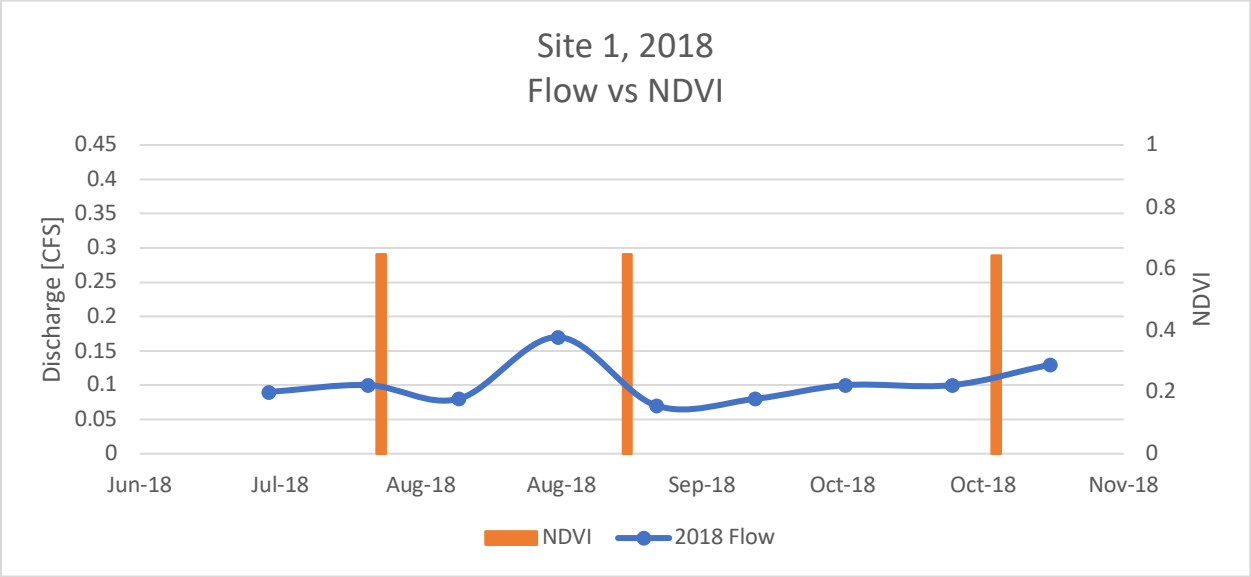

Figure 5. Flow rate and NDVI at Site 1 versus date in 2018.

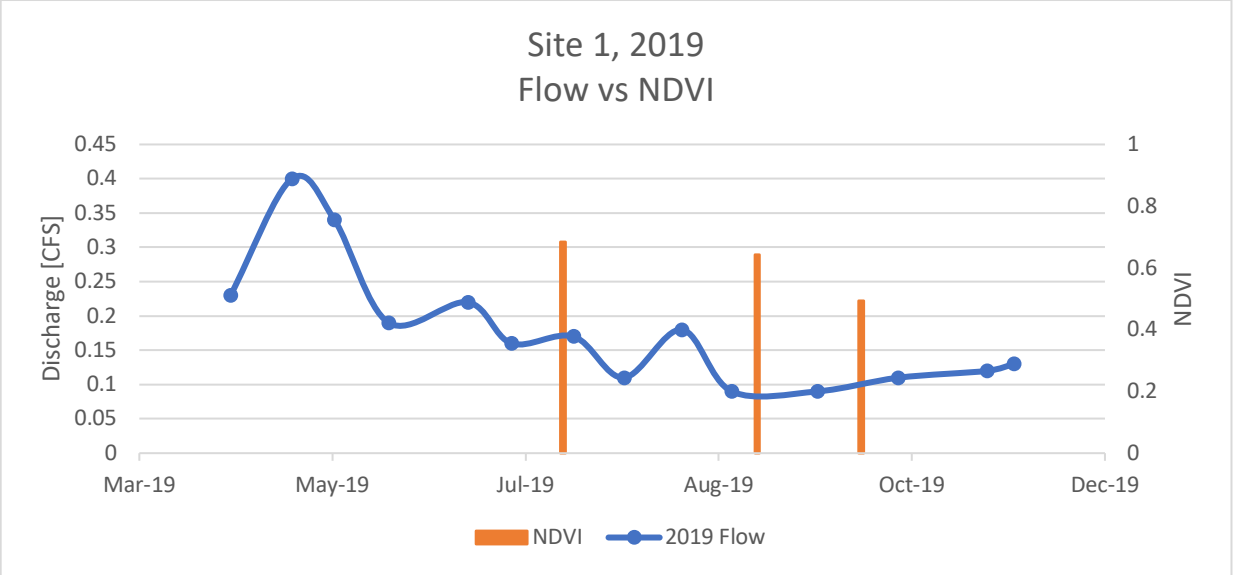

Figure 6. Flow rate and NDVI at Site 1 versus date in 2019.

Site 2

Site 2 shows very little variation in flow rate from month to month throughout the study period, with a maximum change in flow of 0.16 CFS in 2018 (Figure 7), and only 0.07 CFS difference in 2019 (Figure 8). The variance in 2019 is even less if the difference is considered for only the months recorded for both 2019 and 2018, leaving only 0.02 CFS difference between maximum and minimum. The NDVI values trend downward as the months pass, similarly to the Site 1, except for one outlying data point in September 2018, where the NDVI was calculated to be slightly higher, 0.66, compared to lower values in the months surrounding, 0.59 and 0.45. This departure can be attributed to multiple factors including a delayed green-up from a previous precipitation event. This possibility is supported by a small increase in flows recorded in at the site one month prior. However, this is not seen in every situation where flow increases temporarily, so it may be caused by a difference influence.

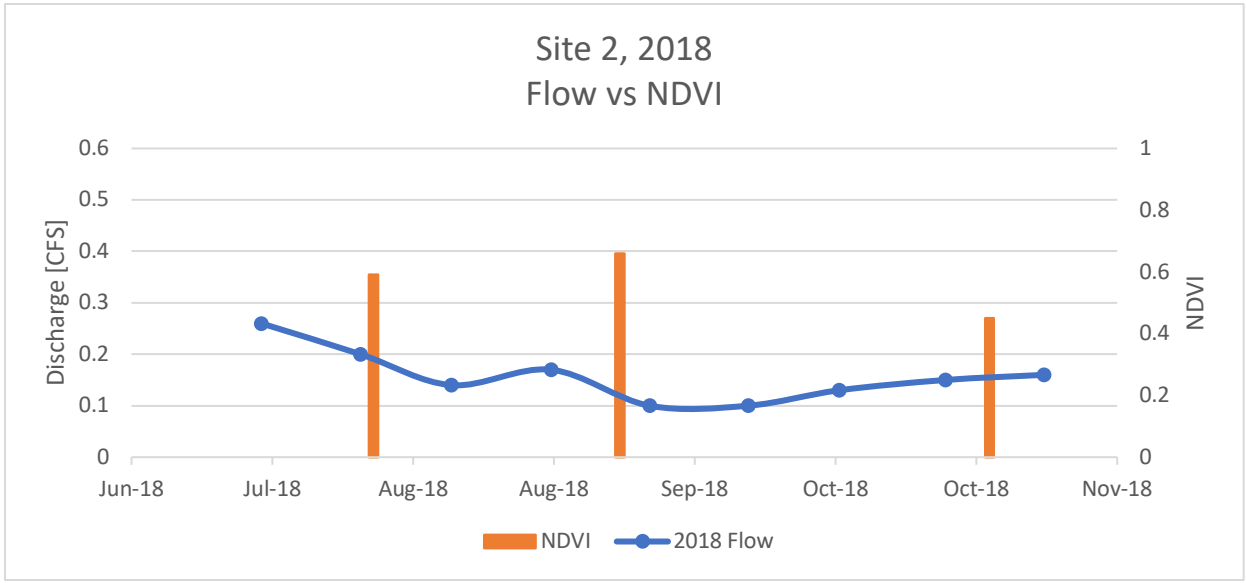

Figure 7. Flow rate and NDVI at Site 2 versus date in 2018.

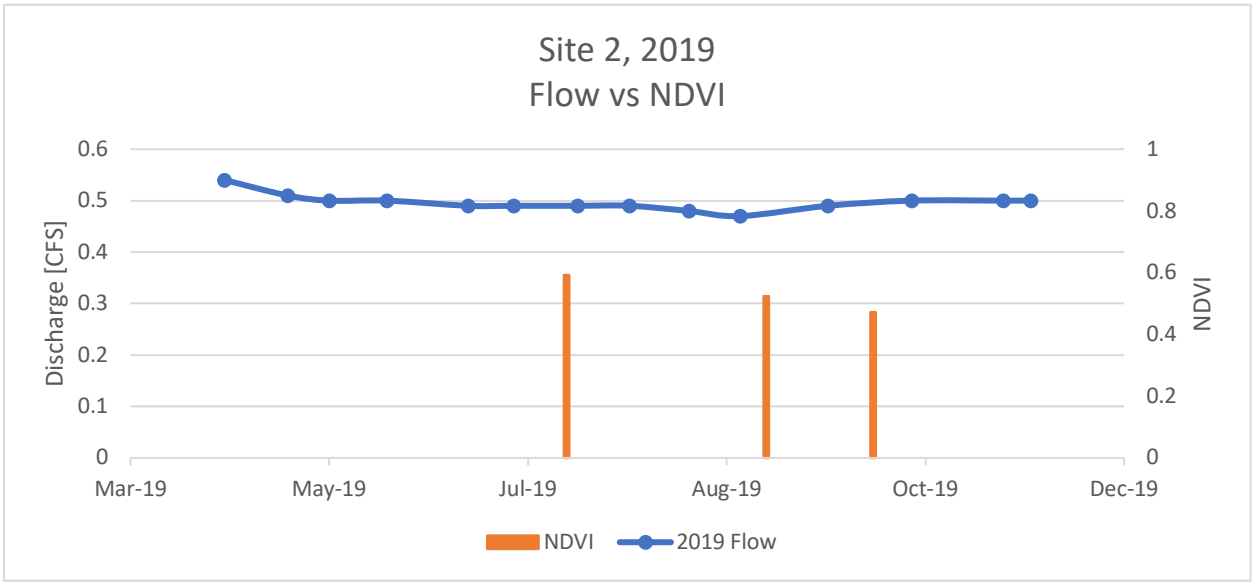

Figure 8. Flow rate and NDVI at Site 2 versus date in 2019.

Site 3

Site 3 is missing flow data from late July and early August due to site accessibility issues. There was a mountain lion in the area causing problems for homeowners, so they asked for site visits to be temporarily cancelled. Other sites above and below Site 3 report generally stable flows during this gap, so it is fair to expect that no major flow events were missed at that time.

Discharge data from 2018 (Figure 9) shows the same gradual decrease in flow over time, mirrored by 2019 data, each decreasing by 0.2 CFS over a similar time period, as shown in Figure 10. NDVI values follow similarly, staying relatively constant, but with a general trend downward throughout the study period.

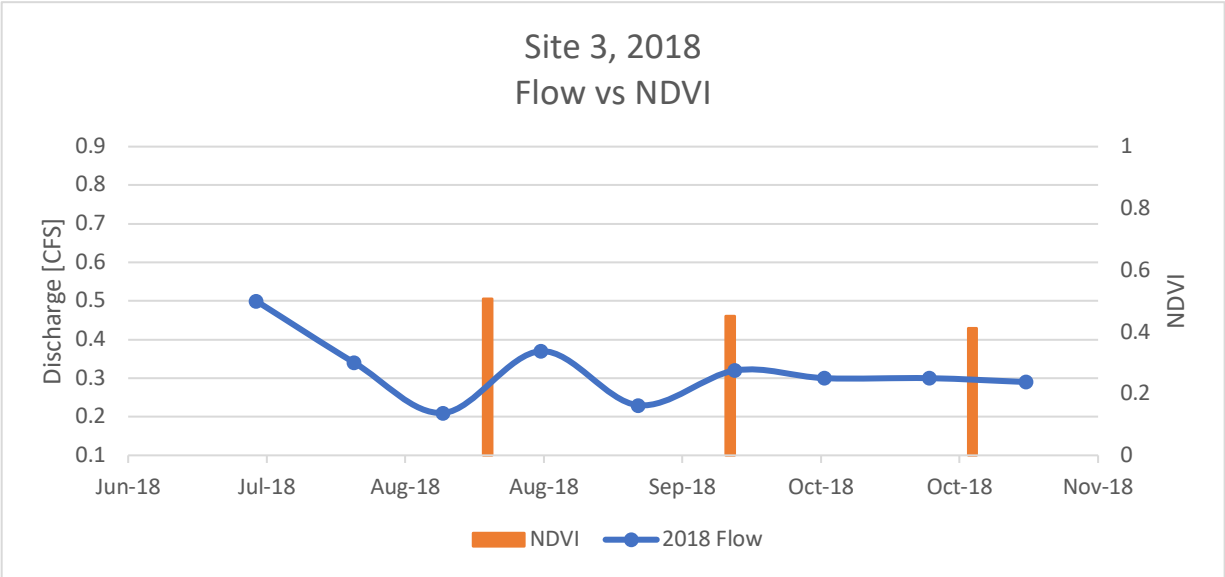

Figure 9. Flow rate and NDVI at Site 3 versus date in 2018.

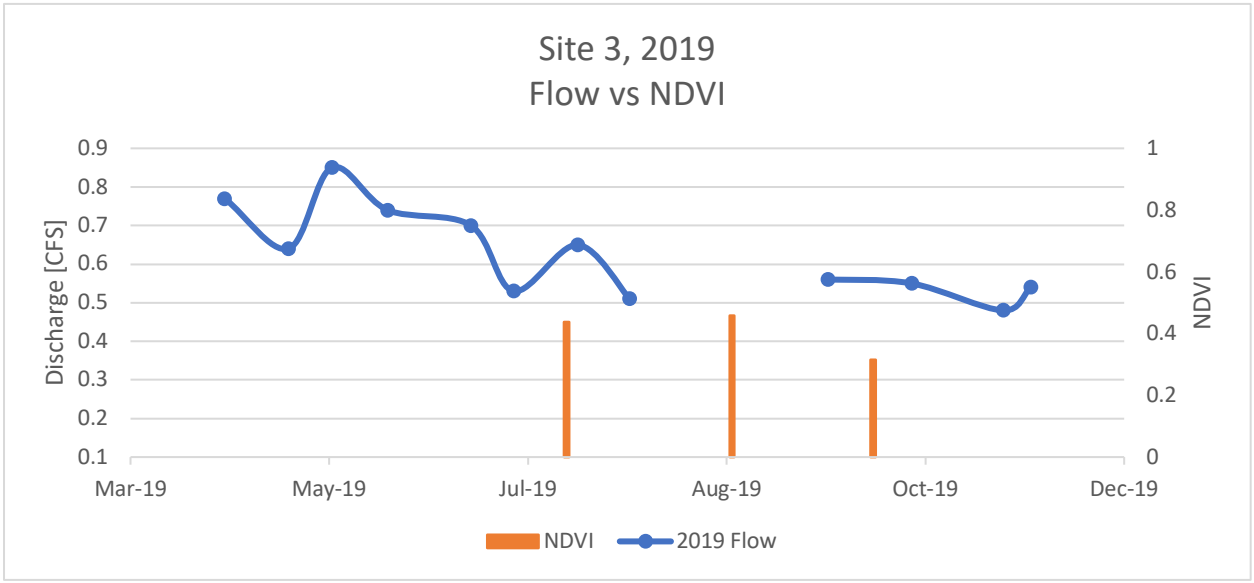

Figure 10. Flow rate and NDVI at Site 3 versus date in 2019.

Site 4

Site 4 is slightly different than each of the preceding sites. It lies just downstream of a diversion that has a portion of its water diverted from Eightmile Creek to another channel, where it flows parallel to the creek and eventually terminates in a privately owned pond. Eightmile Creek at the Site 4 maintains roughly 0.5 feet water depth (which can be considered a moderate stage for this system) throughout this time, however it moves very slowly, resulting in low flow rates. Because of this, flows do not correlate with NDVI as closely as at other sites. NDVI is seen to be fairly steady throughout both study periods, with variations of 0.16 in 2018 (Figure 11) and 0.23 in 2019 (Figure 12). Conversely, flows range more drastically, as much as 0.48 CFS in 2019. This may indicate that the continuously near-standing water remaining in the creek is enough to maintain vegetation greenness in the months when a portion of flows are diverted.

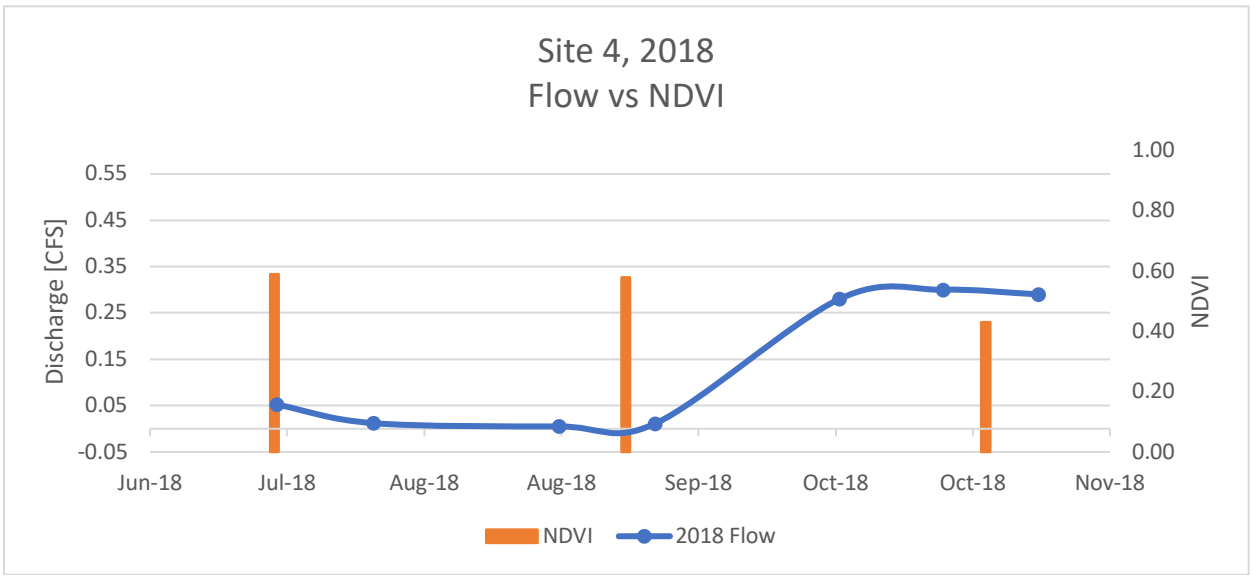

Figure 11. Flow rate and NDVI at Site 4 versus date in 2018.

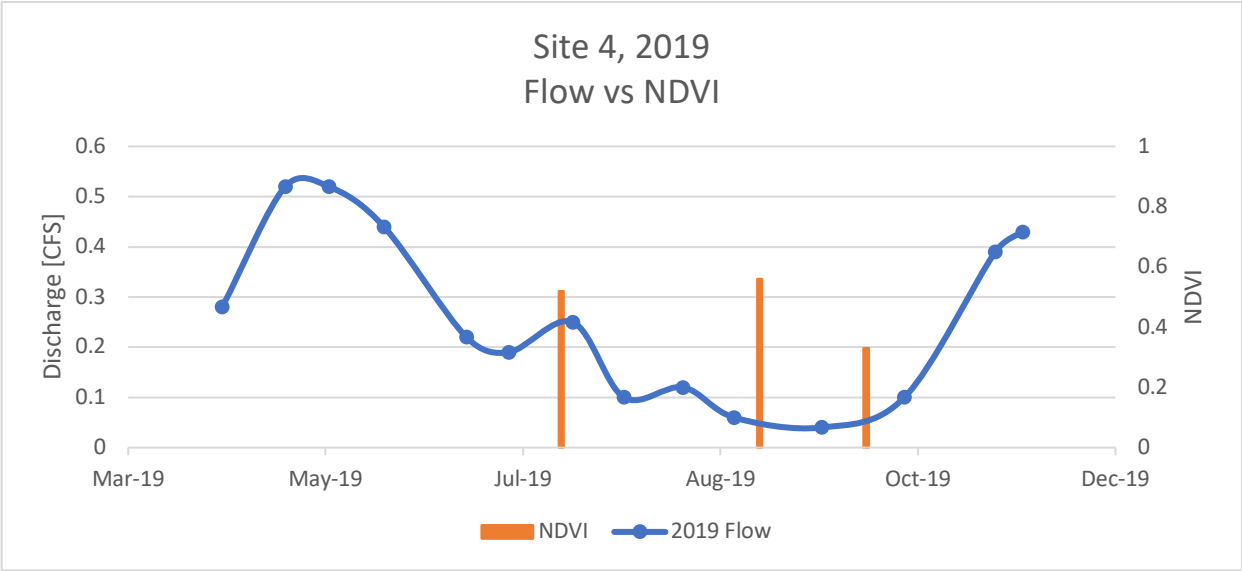

Figure 12. Flow rate and NDVI at Site 4 versus date in 2019.

Site 5

Shown below in Figure 13, Site 5 in 2019 trends downward similarly to the others, with a spike in flow occurring in august 2019, followed by an increase in NDVI values as compared to the surrounding measurements, which may be due to the previous increase in flow. Also, flow increased dramatically in October, after waning to its lowest point, beginning in August. This trough in the flow curve can likely be attributed to the diversion at Site 4 just upstream, which shows a similar drop and gain at the same time. This trend can also be seen in each of the subsequent sites. In 2018, the flows remain steady, ranging 0.17 CFS from July to November, shown in Figure 14. NDVI values are also steadily trending downward toward the fall months.

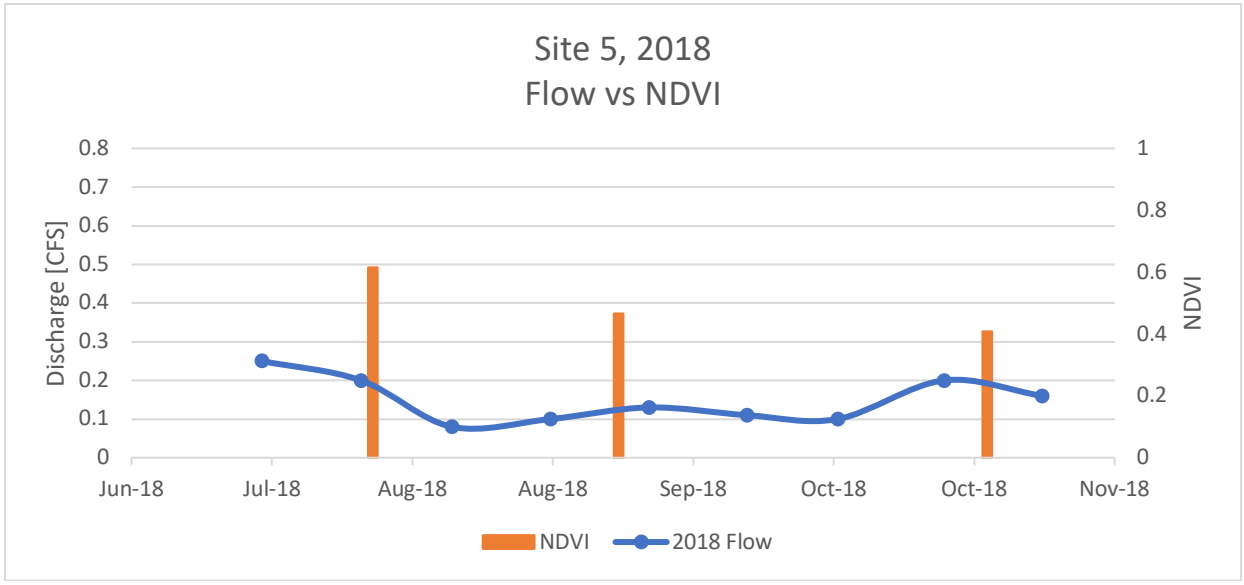

Figure 13. Flow rate and NDVI at Site 5 versus date in 2018.

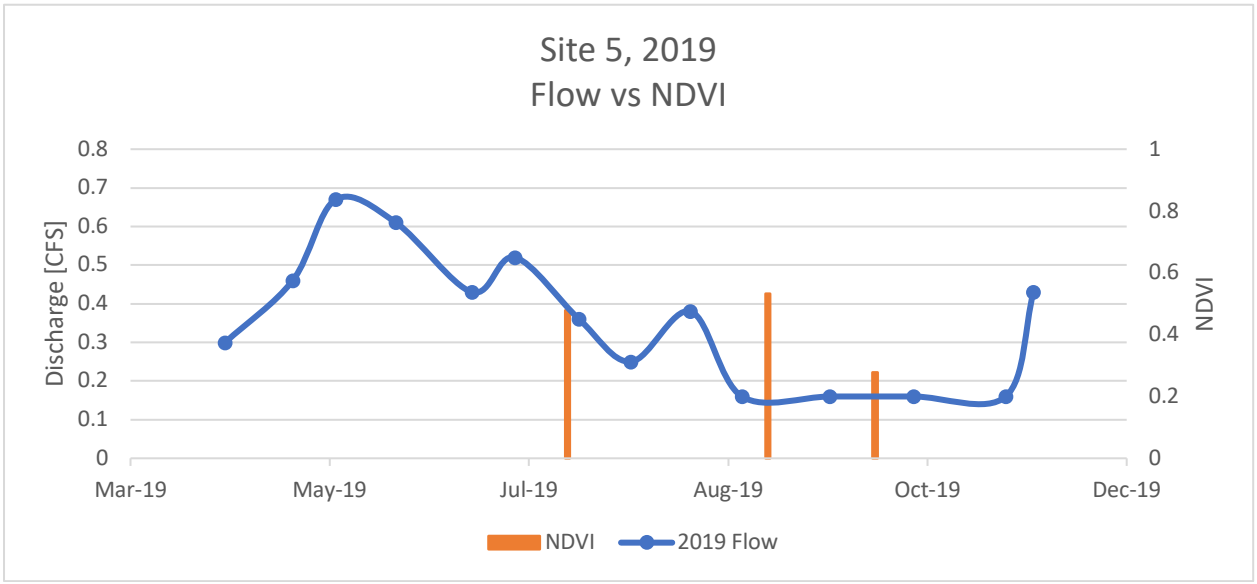

Figure 14. Flow rate and NDVI at Site 5 versus date in 2019.

Site 6

Figure 15 illustrates a decrease in flow at Site 6 from July through August 2018, where it then holds steady for the remainder of the season. NDVI reflects this steadiness, with very little change in calculated values throughout the 2018 study period, shown in Figure 16. Values collected in 2019 show more variation, with a spike in discharge found in August, but no

apparent increase in NDVI values in the weeks following. Increase in October flow coinciding with Site 4 re-diversion is also visible.

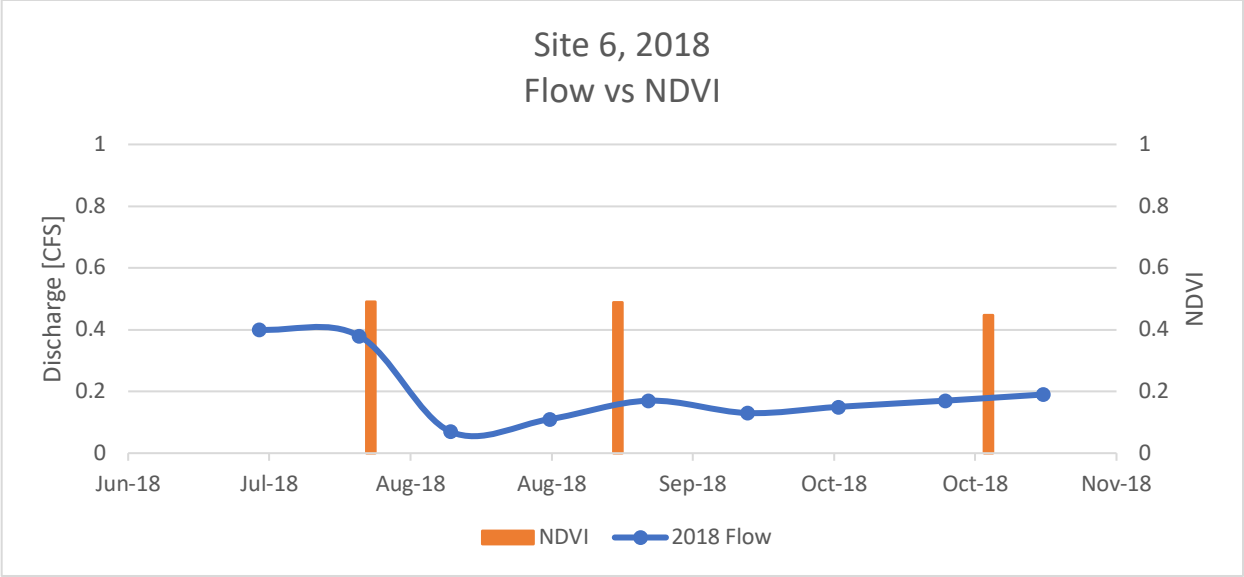

Figure 15. Flow rate and NDVI at Site 6 versus date in 2018.

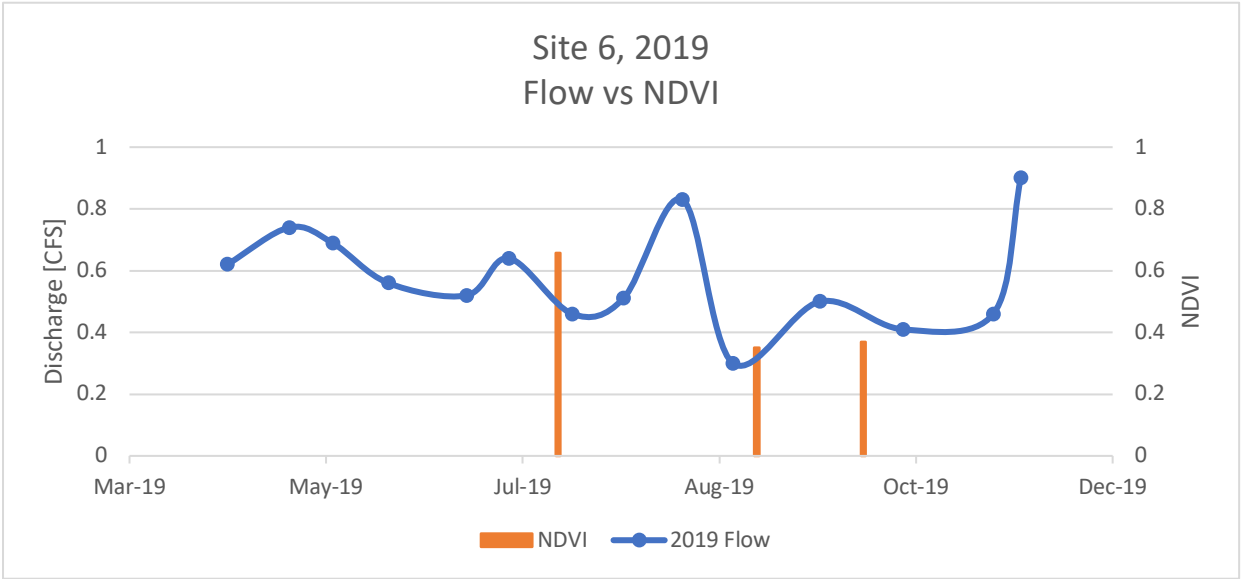

Figure 16. Flow rate and NDVI at Site 6 versus date in 2019.

Site 7

Figure 17 displays a drop in Site 7 flows from July 2018, reaching lowest rates in September, followed by a steady increase until reaching flows equal to those in July. The corresponding NDVI values remain consistent for the duration, ranging between 0.27 and 0.29. Flow values from 2019, shown in Figure 18, show a distinct increase followed by a sharp decrease and subsequent, slower increase. These fluctuations are not reflected strongly in NDVI values, which trend downward then level out. Increase in October flow coinciding with Site 4 re-diversion is also visible, although to a lesser extent than other sites.

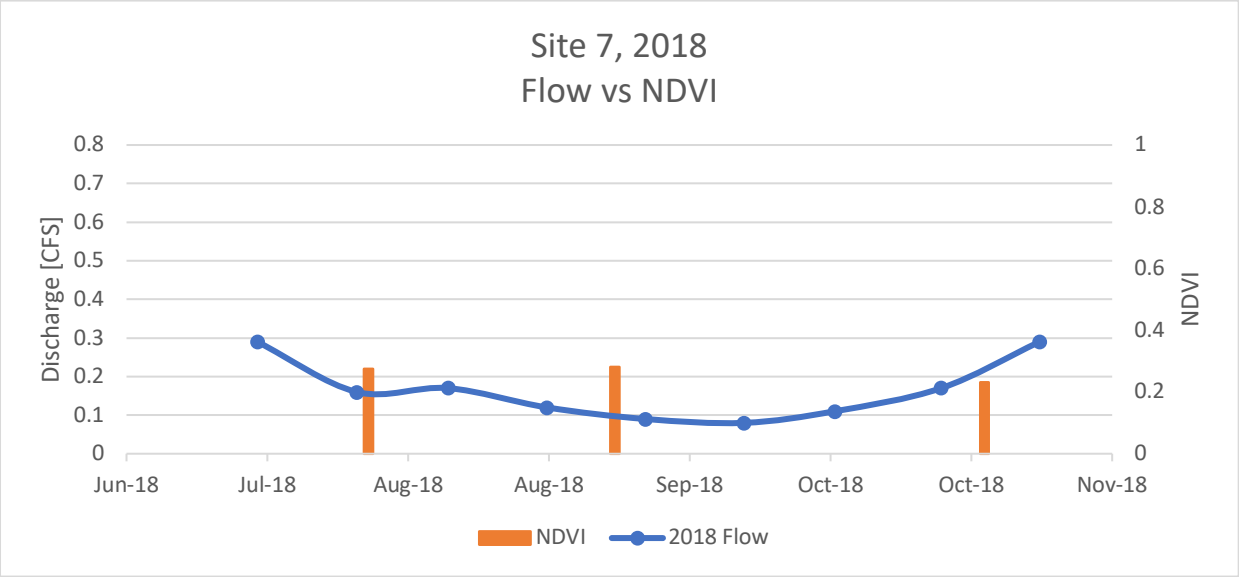

Figure 17. Flow rate and NDVI at Site 7 versus date in 2018.

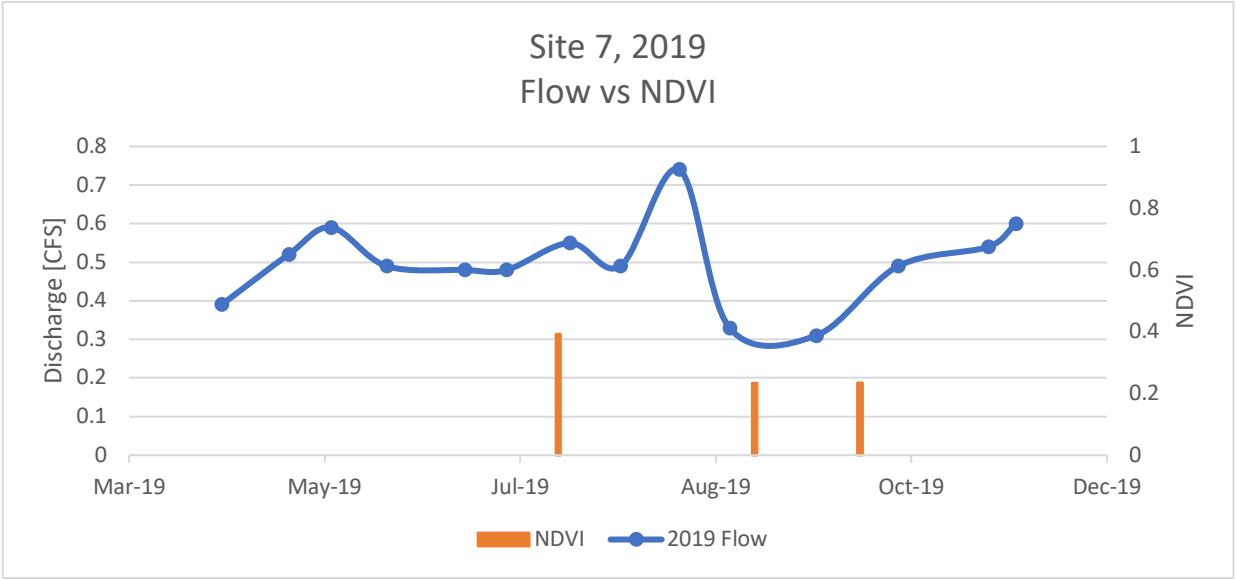

Figure 18. Flow rate and NDVI at Site 7 versus date in 2019.

Site 8

Site 8 behaves similarly in 2018, displayed in Figure 19, with gentle decline then increase in flows, and consistent NDVI values. Figure 20 depicts 2019 values also trend similarly to other sites, with a spike in August, and a steep increase in October corresponding to Site 4 re-diversion. NDVI values however do not appear to be affected by the August pulse of flows.

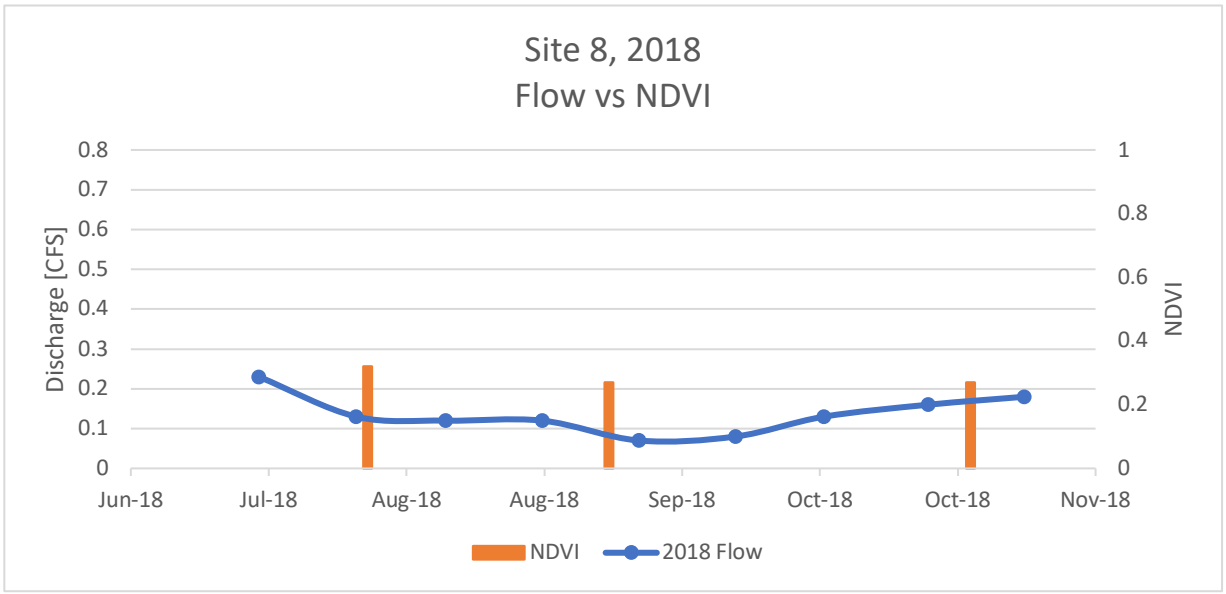

Figure 19. Flow rate and NDVI at Site 8 versus date in 2018.

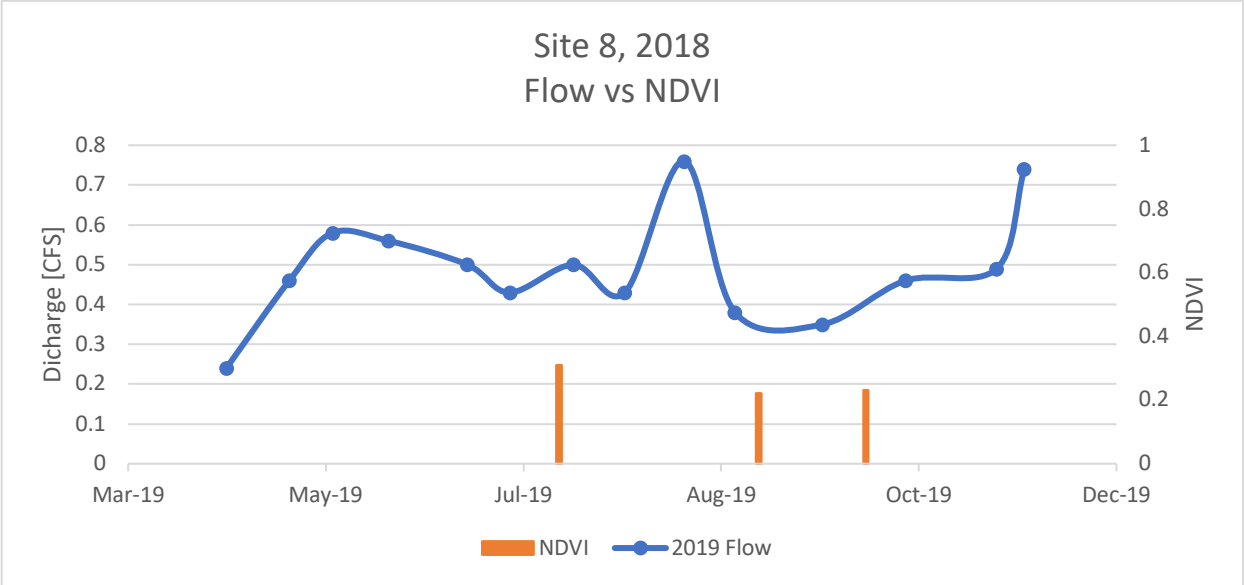

Figure 20. Flow rate and NDVI at Site 7 versus date in 2019.

Discussion & Conclusions

The goals of this project were to use satellite imagery to investigate how vegetation responds in connection with variable stream discharge in the Eightmile Creek watershed prior to significant urbanization. Also, to make predictions and recommendations to mitigate harmful effects of subdividing in semi-arid region. Using a combination of field and remote sensing methods, data were compiled and analyzed for common developments and cause-and-effect patterns while also thinking about the system as a whole, with unique influences, circumstances, and human involvement. Additionally, these data are used to assess implications for restoration.

Linear Regression Analysis

In order to better quantify the relationship between flow rate and NDVI, 2018 and 2019 values of each parameter were plotted and a trendline was fitted to each dataset. Figures 21 and 22, shown below, contain 2018 and 2019 flow rate and NDVI data, respectively. To perform the

linear regression analysis, flow values were approximated using linear interpolation to yield flow rate values representing dates coincident with NDVI measurement dates. The No Delay data sets represent flow rates that have been interpolated to match the dates of the NDVI values to which they are being compared. Two-Week Delay contains the same NDVI values used in the previous set, but with flow values shifted back in time by approximately 2 weeks. Similarly, the Three-Week Delay data use the same NDVI values, and flow values taken from approximately 3 weeks before the NDVI values. 2019 datasets contain a fourth response delay which cannot be found in 2018 data because flow data is not available before mid-July. The shifting frames used are meant to capture the delay that exists between increased moisture presence and the subsequent response from vegetation. The R^2 values obtained from a linear trend line produced by each dataset represent the strength of the connected between flow rate and NDVI for each variation of response time delay plotted.

Table 4, below, summarizes the data used to create a linear regression plot for 2018 NDVI and flow rate data. The dates range from July through October 2018, and contain three time shifts in zero, two, and three-week increments. Columns listed as 'Coincident with NDVI' signify that the flow rate has been interpolated from nearby measurements to reflect likely flow conditions on the same day that the satellite images were taken, from which NDVI values were obtained. This process is necessary in order to perform the linear regression analysis.

Table 4. 2018 Flow rate values organized based on time before NDVI measurement date.

2018	***3 Weeks Before NDVI***		***2 Weeks Before NDVI***		***Coincident with NDVI***		***NDVI***
	Flow Date	Flow Rate [CFS]	Flow Date	Flow Rate [CFS]	Flow Date	Flow Rate [CFS]	
Site 1	7/17/18	0.09	7/31/18	0.10	8/9/18	0.09	0.65
Site 2	7/17/18	0.26	7/31/18	0.20	8/9/18	0.16	0.59
Site 3	7/17/18	0.50	7/31/18	0.34	8/9/18	0.25	0.51
Site 4	7/17/18	0.05	7/31/18	0.01	8/9/18	0.00	0.59
Site 5	7/17/18	0.25	7/31/18	0.20	8/9/18	0.11	0.62
Site 6	7/17/18	0.40	7/31/18	0.38	8/9/18	0.16	0.49
Site 7	7/17/18	0.29	7/31/18	0.16	8/9/18	0.17	0.27
Site 8	7/17/18	0.23	7/31/18	0.13	8/9/18	0.12	0.32
Site 1	8/9/18	0.09	8/27/18	0.17	9/2/18	0.13	0.64
Site 2	8/9/18	0.16	8/27/18	0.17	9/2/18	0.15	0.66
Site 3	8/9/18	0.25	8/27/18	0.37	9/2/18	0.32	0.45
Site 4	8/9/18	0.00	8/27/18	0.01	9/2/18	0.01	0.58
Site 5	8/9/18	0.11	8/27/18	0.10	9/2/18	0.11	0.47
Site 6	8/9/18	0.16	8/27/18	0.11	9/2/18	0.13	0.49
Site 7	8/9/18	0.17	8/27/18	0.12	9/2/18	0.11	0.28
Site 8	8/9/18	0.12	8/27/18	0.12	9/2/18	0.10	0.27
Site 1	9/10/18	0.07	10/7/18	0.10	10/20/18	0.10	0.64
Site 2	9/10/18	0.10	10/7/18	0.13	10/20/18	0.15	0.45
Site 3	9/10/18	0.21	10/7/18	0.30	10/20/18	0.30	0.41
Site 4	9/10/18	0.01	10/7/18	0.28	10/20/18	0.30	0.43
Site 5	9/10/18	0.13	10/7/18	0.10	10/20/18	0.18	0.41
Site 6	9/10/18	0.17	10/7/18	0.15	10/20/18	0.17	0.45
Site 7	9/10/18	0.09	10/7/18	0.11	10/20/18	0.16	0.23
Site 8	9/10/18	0.07	10/7/18	0.13	10/20/18	0.15	0.27

The R^2 values resulting from the 2018 linear regression plot (Figure 21) indicate that these two parameters do not appear to trend strongly with one another. Flow rates found in 2018 were generally lower than those found in 2019, which may contribute to a stronger connection found among 2019 NDVI and flow data, in comparison to 2018 datasets. This could be the result of several issues, most likely due to insufficient flow rates to strongly and noticeably influence NDVI, coupled with limitations associated with the use of very large-scale imaging with coarse

spatial resolution. Problems stemming from limited flow rate data are compounded by the lack of NDVI data available for specific dates at specific intervals. As with the previously discussed methods, this type of analysis could benefit greatly from the use of technology with very fine temporal and spatial resolutions, like drones.

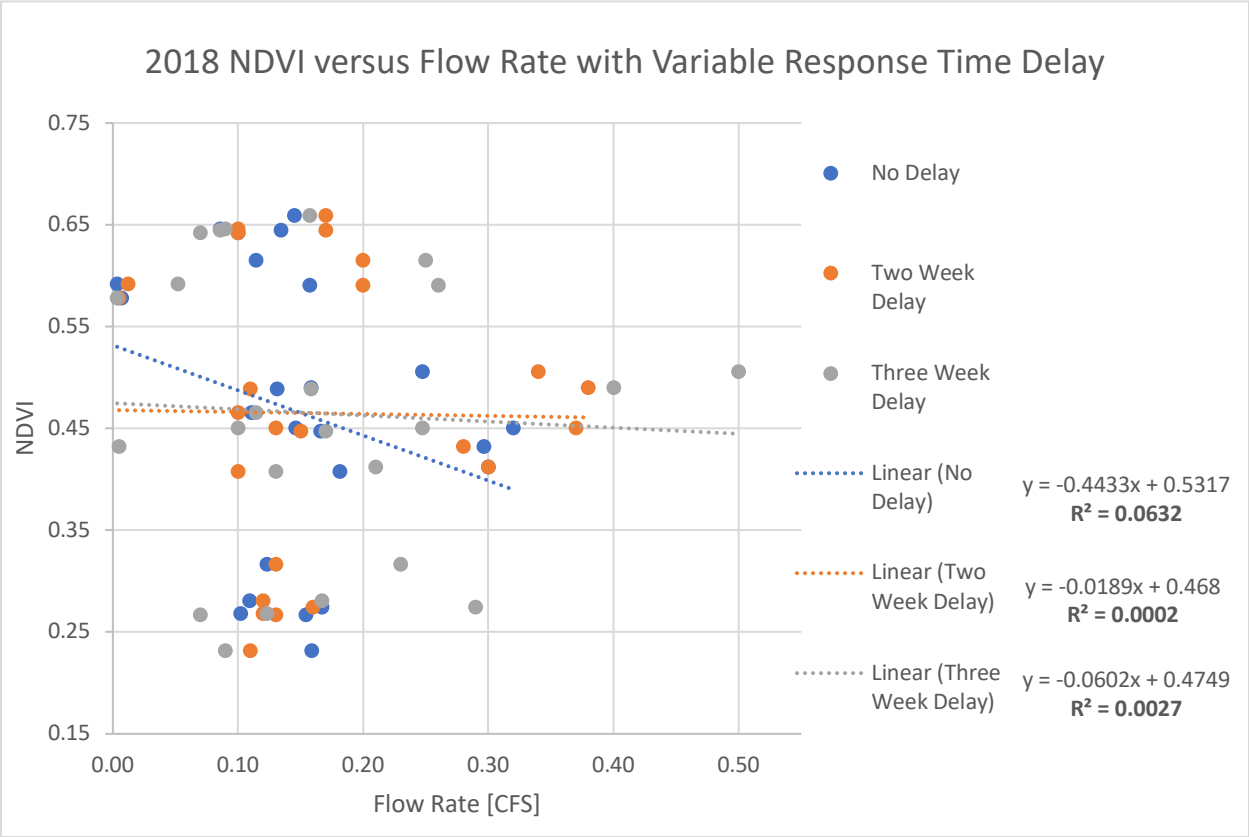

Figure 21. Linear regression plot of 2018 flow rate versus NDVI data.

Table 5, shown below, contains the data used to create Figure 22. It includes flow rate data ranging from May through September 2019 and is organized by the time delay between when flow rate and satellite images (producing NDVI) were taken. The dates listed as two, three, or four weeks prior to NDVI measurements are not exactly that amount of time, rather an approximation of this time lapse.

Table 5. 2019 Flow rate values organized based on time before NDVI measurement date.

2019	***4 Weeks Before NDVI***		***3 Weeks Before NDVI***		***2 Weeks Before NDVI***		***Coincident with NDVI***		***NDVI***
	Flow Date	Flow Rate [CFS]	Flow Date	Flow Rate [CFS]	Flow Date	Flow Rate [CFS]	Flow Date	Flow Rate [CFS]	
Site 1	5/29/19	0.19	6/19/19	0.22	6/30/19	0.16	7/19/19	0.13	0.68
Site 2	5/29/19	0.29	6/19/19	0.29	6/30/19	0.25	7/19/19	0.26	0.59
Site 3	5/29/19	0.74	6/19/19	0.7	6/30/19	0.53	7/19/19	0.55	0.44
Site 4	5/29/19	0.44	6/19/19	0.22	6/30/19	0.19	7/19/19	0.14	0.52
Site 5	5/29/19	0.61	6/19/19	0.43	6/30/19	0.52	7/19/19	0.28	0.48
Site 6	5/29/19	0.56	6/19/19	0.52	6/30/19	0.64	7/19/19	0.50	0.66
Site 7	5/29/19	0.49	6/19/19	0.48	6/30/19	0.48	7/19/19	0.51	0.39
Site 8	5/29/19	0.56	6/19/19	0.5	6/30/19	0.43	7/19/19	0.45	0.31
Site 1	7/16/19	0.17	7/29/19	0.11	8/13/19	0.18	8/28/19	0.09	0.64
Site 2	7/16/19	0.32	7/29/19	0.23	8/13/19	0.23	8/28/19	0.17	0.52
Site 3	7/16/19	0.65	7/29/19	0.51	8/13/19	--	8/28/19	0.51	0.46
Site 4	7/16/19	0.25	7/29/19	0.1	8/13/19	0.12	8/28/19	0.04	0.56
Site 5	7/16/19	0.36	7/29/19	0.25	8/13/19	0.38	8/28/19	0.17	0.53
Site 6	7/16/19	0.46	7/29/19	0.51	8/13/19	0.83	8/28/19	0.50	0.35
Site 7	7/16/19	0.55	7/29/19	0.49	8/13/19	0.74	8/28/19	0.33	0.23
Site 8	7/16/19	0.5	7/29/19	0.43	8/13/19	0.76	8/28/19	0.37	0.22
Site 1	7/29/19	0.11	8/13/19	0.18	8/26/19	0.09	9/5/19	0.09	0.49
Site 2	7/29/19	0.23	8/13/19	0.23	8/26/19	0.2	9/5/19	0.19	0.47
Site 3	7/29/19	0.51	8/13/19	--	8/26/19	--	9/5/19	0.32	0.32
Site 4	7/29/19	0.1	8/13/19	0.12	8/26/19	0.06	9/5/19	0.05	0.33
Site 5	7/29/19	0.25	8/13/19	0.38	8/26/19	0.16	9/5/19	0.17	0.28
Site 6	7/29/19	0.51	8/13/19	0.83	8/26/19	0.3	9/5/19	0.43	0.37
Site 7	7/29/19	0.49	8/13/19	0.74	8/26/19	0.33	9/5/19	0.33	0.23
Site 8	7/29/19	0.43	8/13/19	0.76	8/26/19	0.38	9/5/19	0.38	0.23

Values obtained from Figure 22 trend more strongly in comparison to 2018 data, however never reaching an R^2 value greater than 0.3 suggests that there are still significant sources of uncertainty or variation within the data that is not accounted for by the model. As the time response delay is increased from zero to three weeks, the relationship between the datasets becomes stronger, as seen by the increasing R^2 value. This connection drops off beyond the

three-week delay, indicating that this may be nearing the "sweet spot" for picking up vegetation response to flow rate increases in this system. However, as mentioned earlier, the link is not strong enough to conclude much beyond a moderate connection. Additional data and analysis would be required to further define any influences on the system.

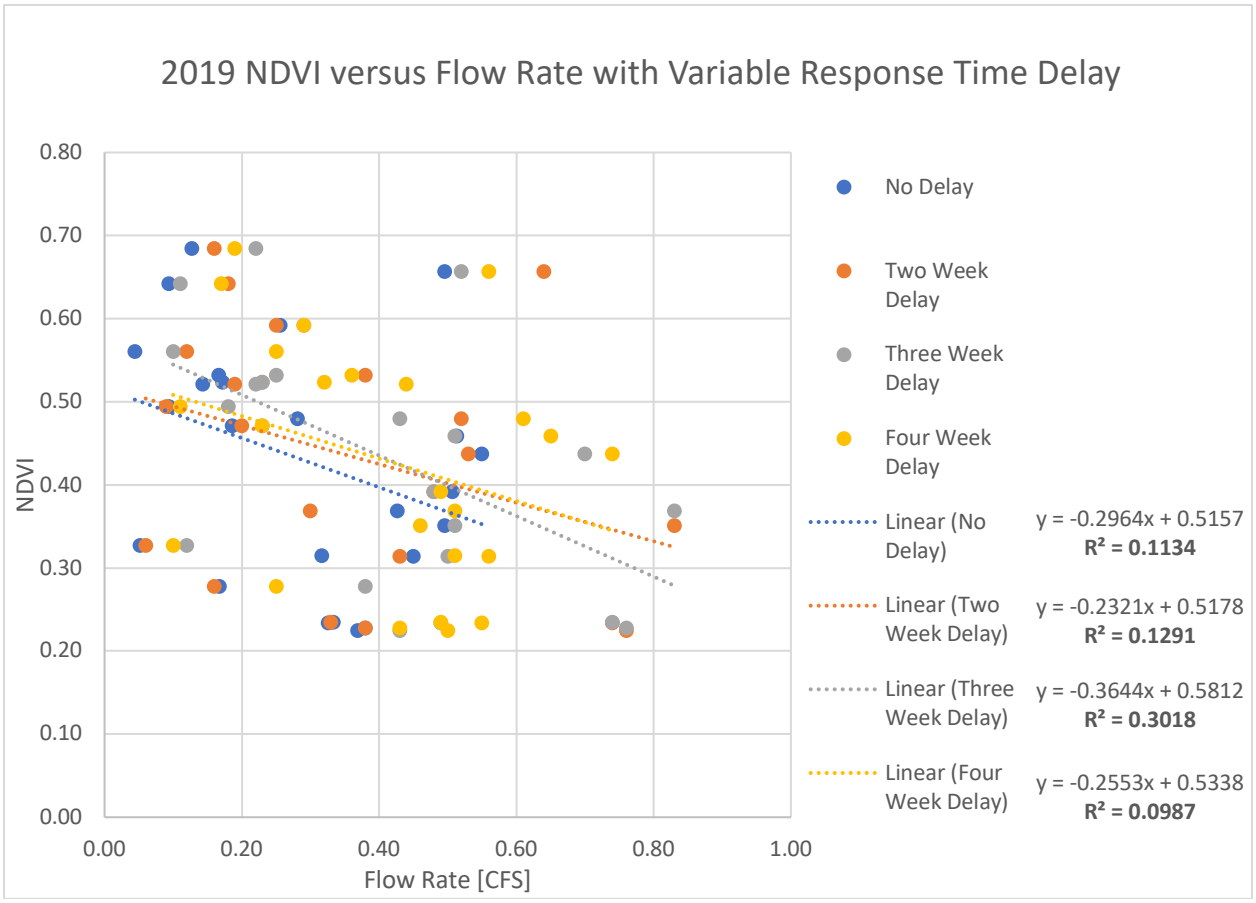

Figure 22. Linear regression plot of 2019 flow rate versus NDVI data.

Vegetation Health, NDVI, and Flow Relationships

As expected, most sites follow a general trend of being greener earlier on in the summer, before heat and dryer months set in. Some sites, however, demonstrate trends indicating the greenness is caused by other factors including local topography, vegetation types, and human

intervention factors. The following sections discuss a breakdown of each of the eight sites, along with their connection or divergence from the expected outcomes.

Site 1 lies the furthest upstream and therefore at the highest elevation on Eightmile Creek, which results in unique conditions at this particular site. NDVI follows the same pattern as at other sites, where it is highest in early summer and continues to drop into fall, however it remains higher than most of the other sites, as shown in Figure 6. The continued greenness found at this site is likely attributable to the density and types of vegetation present, with a mixture of evergreen and deciduous varieties that live closely packed on the hillside. In contrast to other sites that are surrounded solely by grasses, Site 1 does not respond as sharply and remains greener when flows begin to diminish. Results from Site 2 were similar to Site 1, with NDVI values maintaining relatively abundant levels into the fall, as seen in Figure 8. This is expected, as the vegetation present in this area is similar in density immediately surrounding the site, however with fewer evergreen species throughout. Site 3 (Figure 9, Figure 10) continued the trend set by Site 2, but with NDVI values decreasing more rapidly, reaching 0.32 by early fall, likely due to the site being situated in a low-lying area closely surrounded by aspen.

Site 4 departs from the previous sites, with flows decreasing dramatically due to an upstream diversion, but shows only moderate reduction in NDVI, visible in Figure 11 and Figure 12. As mentioned above, this may be due to the presence of nearly half of a foot of near-still water within the channel, even during months when water is diverted. This presence of water allows the area to become saturated, maintaining vegetation health surrounding the stream without significant channel flow.

Site 5 displays the same drop in discharge as Site 4, however NDVI drops along with it, as seen in most clearly in Figure 14. This is likely caused by the lack of bulkier vegetation at this

site, which is surrounded primarily by seasonal grasses that green up significantly in early summer when flows peak and die quickly when temperatures increase. Site 6 behaves very similarly to Site 5, shown in Figure 16, where the drop in flow due to the upstream diversion is visible, followed by a sharp decrease in NDVI. In line with Site 5 results, this site is surrounded by strictly grasses which react strongly to changes in flow, causing this distinct reduction in local photosynthetic activity. Completing the line and continuing the trend, Site 8 also shows the late-summer drop in flow and NDVI, shown in Figure 20. While this site, along with Site 7, displayed the same drop as previous sites, it was not as sharp simply because they were not as intensely green at any point to begin with. These open, treeless areas showed a tendency to explode with new grassland vegetation intermixed with last year's dry remains, which may have diluted the overall NDVI readings for that area.

Overall, the study resulted in a moderate connection between flow and NDVI, indicated by a general downward trend in both parameters as summer months move into fall. However, some anomalous NDVI readings coupled with lack of response from flow increases suggests further inquiry is needed to better define the system and its influences.

Limitations and deficiencies of this study include the coarse grid of Landsat 7 and 8 images, with 30 m by 30 m areas yielding values that may not be precisely reflective of the (rather small) study area. Attempts were made to mitigate this issue by sampling only the pixels corresponding to the exact site location. Similar future endeavors could benefit from the use of more specialized, smaller scale technology, such as drones, to better characterize photosynthesis rates for very small streams like Eightmile Creek. This increased spatial resolution, along with being able to choose days coincident with flow monitoring would help to strengthen connections

found between the two factors. However, the enormous benefit of Landsat images being available free of charge cannot be ignored.

Implications for Restoration

While restoration efforts are generally implemented reactively in an attempt to restabilize a system, it is far more essential that preventative measures are taken to protect an ecosystem from damage, whenever possible. This process can be discussed in the context of Eightmile Creek, and a framework for practical applications to be implemented to mitigate future degradation can be outlined. These actions include erosion control, pollution prevention, biodiversity protection, and ecosystem resilience.

Efforts to control erosion in a small stream system such as Eightmile Creek can be lessened by using several different approaches, likely in a combination rather than one approach alone. The first would be to control surface runoff that may find its way into a stream, uncontrolled. Major precipitation events have the capacity to damage any size stream, and can result in major sediment loss, especially in areas where water is forced between narrower banks, at curves in the stream, or where grade steepens. Methods for mitigating these factors include implementing auxiliary drainage systems that are designed to handle short term pulses of increased flow, moving the excess water away from a small stream, and allowing it to be deposited downstream into a more robust stream or river (Hartup et al., n.d.). Growing areas that are still under development can also set aside areas of centrally located land to be left unpaved so that precipitation is allowed to infiltrate into shallow groundwater systems, thereby lessening the need for runoff management. In areas where this type of infrastructure is not practical or applicable, like Eightmile Creek, more significance shifts toward maintaining presently

occurring vegetation density on the stream banks or increasing density in areas that have become sparse or totally bare. Infiltration capacity in semi-arid grasslands can be supported further by ensuring adequate plant species diversity by way of promoting soil organic carbon content, stability, and porosity (Liu et al., 2019). This suggests that increased species diversity through the use of natural bank stabilization methods can increase infiltration and attenuate the effects of high flow events. Examples of bank stabilization through vegetation techniques include planting willow cuttings in the banks of reaches where willows may typically be found, building live fascines, or using brush layering where necessary.

More than ever, the world is dealing with the consequences of pollution in the forms of acid rain, algal blooms from fertilizer runoff, increased carbon dioxide production, heavy metal contamination, and boundless other examples (U.S. Environmental Protection Agency, 2019). Preventing major sources of pollution to an ecosystem begins by identifying possible contributors, and understanding the ramifications involved. Possible contributions to ecosystem pollution can be as simple as improperly disposing of household cleaning products or could be as complex as industry-scale patterns of disregard for environmental policy. Though these example vary significantly in terms of level of damage, the same steps toward prevention and mitigation can be applied. In the context of Eightmile Creek, possible contributors could be homeowners fertilizing their lawn too aggressively, allowing automotive fluids to leak onto the ground, or even dumping waste into the stream. While these actions may seem insignificant, they can compound over time leaving the system distressed. Steps to avoid these issues would consist of taking proper care to use only as much chemical fertilizer as the land permits, laying down drop cloths to work on a vehicle, and using appropriate waste receptacles for garbage.

Though it may go unnoticed until severe damage has occurred, a system's biological diversity is the backbone of its ability to be resilient and overcome stress (Office of Habitat Conservation, 2020). Protecting biological diversity in the form of animals, plants, invertebrates, and microorganisms is key because it serves as the basis for the food web, regulates nutrient cycles, manages species populations, and fosters a stable and healthy biosphere (Galatowitsch, 2012). Over time, an endless barrage of overexploitation, pollution, invasive species introduction, climate irregularity, or improper land management can result in reduced or completely demolished biological diversity networks. In order to repair a system or to prevent further harm, one must first study how the system may have been irrevocably altered by the damage, by what, and if it can be removed or undone. An example of this occurring within Eightmile Creek may come in the form of an invasive species of plant being introduced to the system, which could result in increased competition for resources, leading to the habitat being overtaken by the newly introduced species, displacing native species. This very scenario has occurred all over the globe and is usually not able to be completely reversed. According to the USDA, invasive species tend to thrive in newly introduced environments because they often contain vast quantities of seed, live easily disturbed soil, have aggressive root systems, and can even give off chemicals that inhibit the growth of competing species (U.S. Department of Agriculture, n.d.). In light of these issues, it is imperative that the propagation of native species is facilitated whenever possible, and the introduction of foreign species is limited.

A final method of protecting a stream habitat is by strengthening its resilience in response to drivers and stressors by maintaining a healthy environment. Ecosystems have a greater capacity for resilience if they are intact, meaning there has not been a major degradation of key factors like biodiversity, water and soil quality and hydrological stability (Galatowitsch, 2012).

This is especially applicable to Eightmile Creek, because it is presently functioning independently and consistently. In the event of a disturbance, there is a strong probability that the stream and its ecosystem would be capable of recovering from the stress event. For a stream that has experienced a disturbance and has not recovered, it may then become necessary to intervene. However, the end goal is still the same: to have the system support itself without outside interference. If a wetland restoration project requires yearly re-plantings of all vegetation, it may be an indication that the method being used needs to be reworked. While there will always be instances where areas of plants simply do not take, or species do not thrive immediately, it's important to recognize that an assortment of restoration techniques will nearly always be required.

References

Alig, R. J., Kline, J. D., & Lichtenstein, M. (2004). Urbanization on the US landscape: looking ahead in the 21st century. Landscape and Urban Planning, 219-234.

Galatowitsch, S. M. (2012). Ecological Restoration. Sunderland: Sinauer Associates, Inc.

Hartup, W., Lord, B., Patoprsty, W., Woodward, M., & Woofter, S. (n.d.). Small-scale Solutions to Eroding Streambanks. NC State University and A&T State University Cooperative Extension.

Kellog, Karl S., Ruleman, Chester A., Vuke, Susan M. "Geologic map of the central Madison Valley (Ennis area) Southwestern Montana." *MBMG Open File Report 543*, Montana Bureau of Mines and Geology, 2007, www.mbmg.mtech.edu/pdf-open-files/mbmg543-centralmadison.pdf.

Liu, Y., Miao, H.-M., Chang, X., & Wu, G.-L. (2019). Higher species diversity improves soil water infiltration capacity by increasing soil organic matter content in semiarid grasslands. Land Degradation & Development, 1599-1606.

Montana Bureau of Mines and Geology. (2020). GWIC Well Data. Retrieved from the Ground Water Information Center: https://mbmggwic.mtech.edu/

Mueggler, W. F., & Stewart, W. L. (1980). Grassland and shrubland habitat types of Western Montana. Ogden, Utah: USDA Forest Service.

National Water and Climate Center. (n.d.). Automated Snow Monitoring. Retrieved from Natural Resource Conservation Service: https://www.wcc.nrcs.usda.gov/about/mon_automate.html

Odeh, T., Mohammad, A. H., Hussein, H., Ismail, M., & Almomani, T. (2019). Over-pumping of groundwater in Irbid governorate, northern Jordan: a conceptual model to analyze the

effects of urbanization and agricultural activities on groundwater levels and salinity. Environmental Earth Sciences.

Office of Habitat Conservation. (2020). River Habitat. Retrieved from NOAA Fisheries: https://www.fisheries.noaa.gov/national/habitat-conservation/river-habitat

Pérez-Pérez, M., Martínez Sánchez, A., de Luis Carnicer, P., & José Vela Jiménez, M. (2004). A technology acceptance model of innovation adoption: The case of teleworking. European Journal of Innovation Management, 7(4), 280–291. https://doi.org/10.1108/14601060410565038

Sabins, F. F. (2007). *Remote Sensing Principles and Interpretation.* Long Grove: Waveland Pressing, Inc.

Shama, Charles, "Mountain front recharge in a semi-arid climate, Southwest Montana" (2018). Graduate Theses & Non-Theses. 161. https://digitalcommons.mtech.edu/grad_rsch/161

United States Census Bureau. (2020). City and Town Population Totals: 2010 - 2019. Retrieved from https://www.census.gov/data/tables/time-series/demo/popest/2010s-total-cities-and-towns.html

U.S. Department of Agriculture. (n.d.). Invasive Plants. Retrieved from U.S. Forest Service: https://www.fs.fed.us/wildflowers/invasives/index.shtml

U.S. Environmental Protection Agency. (2019, November 18). Pollution Prevention (P2). Retrieved from EPA: https://www.epa.gov/p2/learn-about-pollution-prevention

U.S. Geological Survey (n.d.) Landsat Surface Reflectance-Derived Spectral Indices. https://www.usgs.gov/land-resources/nli/landsat/landsat-normalized-difference-vegetation-index?qt-science_support_page_related_con=0#qt-science_support_page_related_con

Viviroli, D., Dürr, H., Messerli, B., Meybeck, & M., Weingartner, R. (2007). Mountains of the world, water towers for humanity: Typology, mapping, and global significance. Water Resources Research. 43. 10.1029/2006WR005653.

Western Regional Climate Center (n.d.). Ennis, Montana—Climate summary. Retrieved November 25, 2020, from https://wrcc.dri.edu/cgi-bin/cliMAIN.pl?mtenni